Developmental Cell
Article

Polar Body Emission Requires a RhoA Contractile Ring and Cdc42-Mediated Membrane Protrusion

Xuan Zhang,[1,5] Chunqi Ma,[1,5] Ann L. Miller,[2] Hadia Arabi Katbi,[1,3] William M. Bement,[2] and X. Johné Liu[1,3,4,*]
[1]Ottawa Health Research Institute, Ottawa Hospital, 725 Parkdale Avenue, Ottawa, ON K1Y 4E9, Canada
[2]Department of Zoology, University of Wisconsin-Madison, 1117 West Johnson Street, Madison, WI 53706, USA
[3]Department of Biochemistry, Microbiology and Immunology
[4]Department of Obstetrics and Gynecology
University of Ottawa, Ottawa, ON K1N 6N5, Canada
[5]These authors contributed equally to this work
*Correspondence: jliu@ohri.ca
DOI 10.1016/j.devcel.2008.07.005

SUMMARY

Vertebrate oocyte maturation is an extreme form of asymmetric cell division, producing a mature egg alongside a diminutive polar body. Critical to this process is the attachment of one spindle pole to the oocyte cortex prior to anaphase. We report here that asymmetric spindle pole attachment and anaphase initiation are required for localized cortical activation of Cdc42, which in turn defines the surface of the impending polar body. The Cdc42 activity zone overlaps with dynamic F-actin and is circumscribed by a RhoA-based actomyosin contractile ring. During cytokinesis, constriction of the RhoA contractile ring is accompanied by Cdc42-mediated membrane outpocketing such that one spindle pole and one set of chromosomes are pulled into the Cdc42 enclosure. Unexpectedly, the guanine nucleotide exchange factor Ect2, which is necessary for contractile ring formation, does not colocalize with active RhoA. Polar body emission thus requires a classical RhoA contractile ring and Cdc42-mediated membrane protrusion.

INTRODUCTION

Polar body emission during vertebrate oocyte maturation is an extreme form of asymmetric cell division (Maro and Verlhac, 2002). In *Xenopus* oocytes, approximately 2 hr following germinal vesicle (nuclear envelope) breakdown (GVBD), the metaphase I spindle assumes a highly asymmetric position with one pole anchored to the animal pole cortex. In the span of 10–15 min, synchronous separation of chromosome homologs occurs, followed by lopsided cytokinesis to emit a polar body with a complete set of chromosome homologs and minimum cytoplasmic content. The condensed egg chromosomes are then organized into a metaphase II spindle without nuclear envelope reformation, and the spindle again assumes the same asymmetric configuration, approximately 3 hr following GVBD (Gard, 1992; Ma et al., 2006).

Maturation promoting factor (MPF) (Masui and Markert, 1971), a complex of cyclin-dependent protein kinase 1 (Cdk1) and cyclin B (Gautier et al., 1990), is thought to be the key enzyme controlling oocyte maturation. In *Xenopus* oocytes, the steroid hormone progesterone activates a signaling cascade that culminates in abrupt MPF activation (Masui and Markert, 1971) at the time of GVBD. Within 30 min of GVBD, however, the level of MPF activity is transiently and partially reduced (Gerhart et al., 1984), due to polyubiquitination-mediated proteolysis of its regulatory subunit, cyclin B (Hochegger et al., 2001). The second phase of MPF activity increase occurs as a result of de novo synthesis of cyclin B, approximately 2.5 hr after GVBD (Hochegger et al., 2001; Mendez et al., 2002), coinciding with the oocyte's entering metaphase II arrest (Gerhart et al., 1984; Ma et al., 2003). Therefore the first phase of MPF activation drives the oocyte into metaphase I and the second phase is responsible for metaphase II entry and arrest. The partial (instead of complete) inhibition of MPF appears to be uniquely required to prevent reformation of the nuclear envelope, as well as to inhibit DNA replication between metaphase I and metaphase II (Iwabuchi et al., 2000).

We recently demonstrated that activation of the small G protein Cdc42 is required for cytokinesis during first polar body emission in *Xenopus* oocytes. Cdc42 is first activated at the spindle pole-cortex contact site at the start of cytokinesis. The activity zone of Cdc42 defines the inner boundary of a ring of Rho A activity; the latter patterns the cytokinetic contractile ring (Ma et al., 2006). Inhibition of Cdc42 activation, with a dominant-negative Cdc42 mutant (Cdc42N17), abolishes first polar body emission by inhibiting cytokinesis without affecting asymmetric spindle positioning or chromosome separation. In the current study, we have addressed two questions: (1) How is activation of Cdc42 regulated? (2) How does Cdc42 activity coordinate with RhoA activity in controlling the contractile ring? Our data support the following conclusions: (1) Perpendicular configuration of the metaphase I spindle at the onset of anaphase is required for Cdc42 activation. (2) Polyubiquitin-mediated cyclin B degradation is required for anaphase I and subsequent Cdc42 activation. (3) The guanine nucleotide exchange factor, Ect2, is required for RhoA contractile ring formation. (4) Cdc42 and RhoA form mutually exclusive activity zones during polar body emission through both stimulatory and inhibitory interactions. (5) Cdc42 and RhoA make distinct contributions to the process of polar body emission: RhoA templates formation of the contractile ring, which is enriched in myosin-2 and stable F-actin and which drives contraction, while Cdc42 templates a cap of highly dynamic F-actin

that defines the surface of the forming polar body and undergoes outpocketing.

RESULTS

Cyclin B Degradation Is Required for Anaphase Initiation and for Cdc42 Activation

Cdc42 activation is first observed at the spindle-cortex contact site shortly (within a few minutes) following anaphase initiation (Ma et al., 2006), suggesting that activation of Cdc42 might be temporarily and mechanistically coupled to anaphase. We wished to inhibit anaphase without altering spindle assembly or the perpendicular spindle attachment to the oocyte cortex. The role of cyclin B degradation and the resultant loss of Cdk1 activity during amphibian meiosis is controversial. While it has been reported that stabilization of Cdk1 activity via prevention of cyclin B destruction does not prevent polar body formation (Taieb et al., 2001; Peter et al., 2001), it has also been reported that experimental stabilization of Cdk1 by other means does block polar body emission and that this blockade can be relieved by Cdk1 inhibition (Gorr et al., 2006). We therefore reinvestigated the role of cyclin B degradation on polar body emission. We employed a truncated form of cyclin B1 (ΔN cyclin B1 [Gross et al., 2000]) that lacks the destruction box required for APC-targeted degradation, as opposed to the destruction peptide employed by Peter et al. (2001). Injection of ΔN cyclin B1 mRNA efficiently eliminated the transient inactivation of MPF seen in control oocytes (Figure 1A). Oocytes injected with ΔN cyclin B1 underwent progesterone-induced GVBD indistinguishably from control oocytes (data not shown). However, oocytes injected with ΔN cyclin B1 mRNA failed to emit the first polar body (Figure 1B). Similarly, injection of methylubiquitin effectively inhibited cyclin B degradation (see Figure S1A available online) and inhibited first polar body emission (Figure S1B).

We next carried out time-lapse imaging (or 4D imaging [Bement et al., 2003]) experiments to determine the effect of ΔN cyclin B1 on Cdc42 activation in live oocytes, using eGFP-wGBD, a GFP fusion protein containing the GTPase-binding domain of WASP (wGBD) that binds only active (GTP-bound) Cdc42 (Sokac et al., 2003). As shown previously (Ma et al., 2006), control oocytes exhibited Cdc42 activation approximately 2 hr after GVBD, emitted the first polar body, and then arrested in metaphase II indefinitely (Figure 1C, top row, and Movie S1). In contrast, ΔN cyclin B1-injected oocytes failed to activate Cdc42, and the spindle remained intact and attached to the cortex for an extended period of time (Figure 1C, bottom row, and Movie S2). Similarly, methylubiquitin-injected oocytes exhibited intact metaphase I spindles that remained asymmetrically attached to the cortex, with no Cdc42 activation (Figure S1C).

Given the controversy regarding whether the transient degradation of cyclin B is required for homolog separation in *Xenopus* oocytes (Peter et al., 2001; Taieb et al., 2001), we wished to observe chromosome dynamics in live oocytes injected with ΔN cyclin B1 mRNA. We employed fluorescent antibodies against *Xenopus* Aurora B (see Experimental Procedures) to track endogenous Aurora B, a chromosome passenger kinase (Rogers et al., 2002). As shown in Figure 1D (and Movies S3 and S4), fluorescent anti-Aur B faithfully tracked chromosomes through the metaphase I (00:10) to metaphase II (00:52) transition. In addition, fluorescent anti-Aur B also clearly marked the central spindle or spindle midzone (MZ) at anaphase/telophase (arrows, 00:20–00:24), and the midbody following polar body emission (arrow, 00:28). These data are consistent with previous conclusions based on staining of fixed oocytes of other species (Rogers et al., 2002; Uzbekova et al., 2008). It is noteworthy that in contrast to mitosis in which Aurora B is completely transferred to the central spindle at anaphase (Ruchaud et al., 2007), in the oocytes Aurora B persisted with the segregated chromosome homologs (Figure 1D) (Rogers et al., 2002). Presumably, Aurora B signal persisted at anaphase I due to the cohesion of sister centromeres, which only resolve at anaphase II upon fertilization (Kudo et al., 2006).

Having established the utility of fluorescent anti-Aur B in tracking chromosomes in live oocytes, we followed the fate of chromosomes in oocytes injected with ΔN cyclin B1. As shown in Figure 1E, metaphase I spindles remained asymmetrically positioned against the animal pole cortex for an extended period of time, with no homolog separation. Similarly, oocytes injected with methylubiquitin did not separate chromosome homologs (data not shown). These data clearly indicate that cyclin B degradation is required for anaphase initiation and for Cdc42 activation.

Securin Degradation Is Required for Homolog Separation but Not for Spindle Changes during Anaphase

To directly assess whether homolog separation is required for Cdc42 activation, we employed a D box mutant of *Xenopus* Securin (xSecurin^{dm}) to inhibit *Xenopus* separase (Zou et al., 1999). Injection of mRNA encoding xSecurin^{dm} did not interfere with progesterone-induced GVBD (data not shown). Importantly, oocytes injected with xSecurin^{dm} also exhibited the typical biphasic pattern of MPF activity (Figure 2A) found in control oocytes, indicating that xSecurin^{dm} did not interfere with cyclin B degradation. However, when these oocytes were fixed and examined for chromosome morphology, it became clear that they too failed to emit the first polar body (Figure 2B). To further characterize the effect of xSecurin^{dm} on oocyte maturation, we carried out live oocyte imaging experiments. Although, as expected, chromosome separation did not occur (Figure 2C and Movie S5), metaphase I spindles in xSecurin^{dm}-injected oocytes underwent dramatic shortening (00:15–00:24), indicative of ''anaphase A'' in which kinetochore microtubules progressively shorten. In the absence of homolog separation, the spindle eventually resumed its normal length (00:48). We often observed some chromosomes (presumably unresolved chromosome bivalent[s]) break away temporarily (arrow, 00:33) but quickly rejoin the rest when the metaphase spindle reassembled, similar to the results previously obtained in mouse oocytes lacking separase (Kudo et al., 2006). These results are in contrast to those in oocytes injected with methylubiquitin or ΔN cyclin B1 in which metaphase I spindle remained unchanged.

To determine whether Cdc42 activation occurred in xSecurin^{dm} -injected oocytes, we carried out time-lapse imaging experiments. We consistently observed a small Cdc42 activity zone at the center of the spindle pole during the period of spindle shortening, but this Cdc42 activity zone never expanded into a robust cap (Figure 2D, lower row, and Movie S7), as it did in control

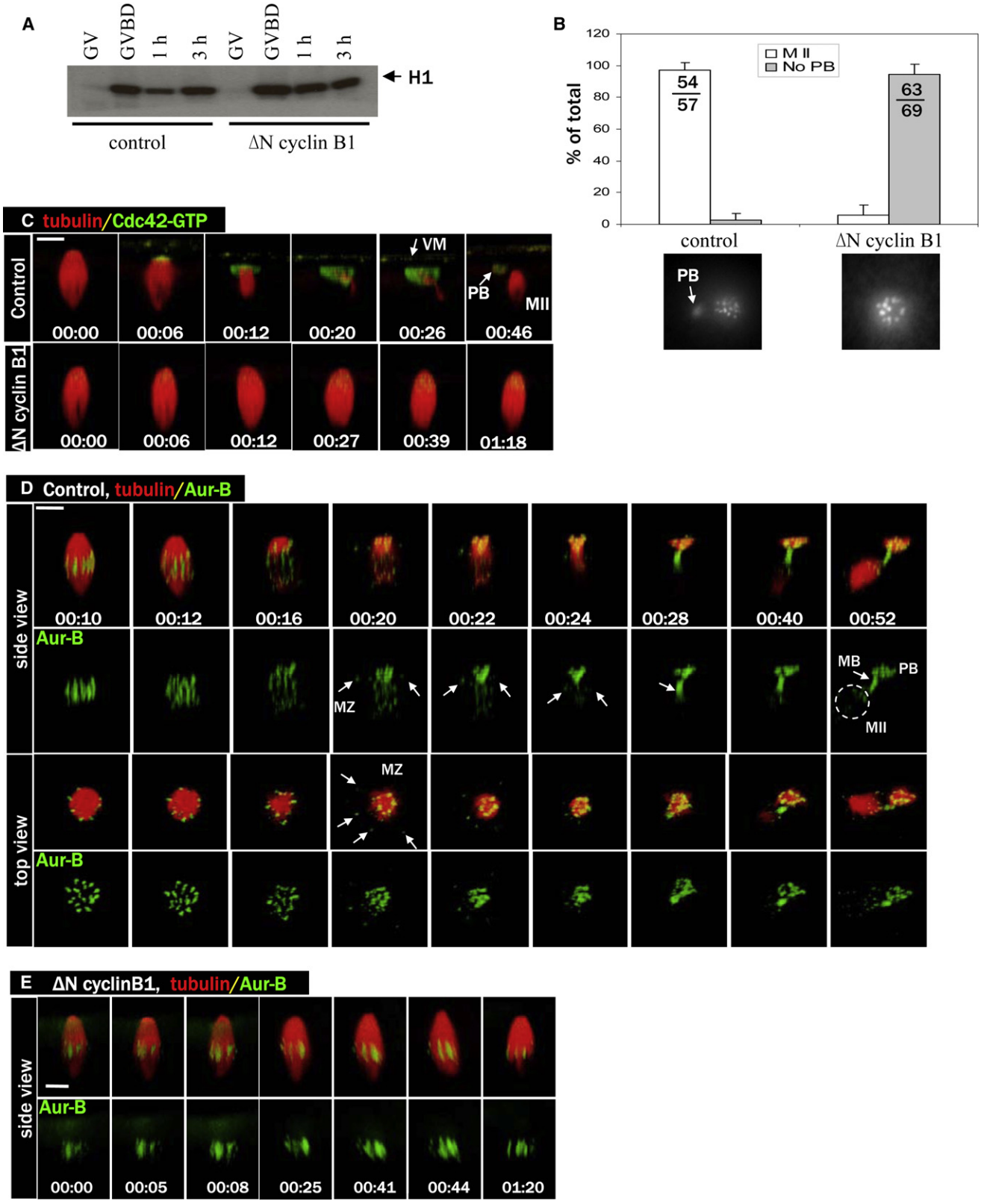

Figure 1. Cyclin B Degradation Is Required for Anaphase Initiation and for Cdc42 Activation

(A) Control oocytes and oocytes injected with ΔN cyclin B1 mRNA were incubated with progesterone and withdrawn at GVBD, or 1 or 3 hr after GVBD, for MPF (histone H1 kinase) assays. GV oocytes were not treated with progesterone. Note the transient (1 hr) inactivation of MPF in control but not ΔN cyclin B1 oocytes.

oocytes (Figure 2D, upper row, and Movie S6), and disappeared when the metaphase I spindle reassembled (we call this the metaphase I spindle because chromosome homolog separation never occurred; see above). These results clearly indicated that, similarly to mitosis and meiosis in other organisms, homolog separation in meiosis I in *Xenopus* oocytes requires Securin degradation. These results also suggest that Cdc42 activation is coupled to spindle changes during anaphase and not to homolog separation per se.

Asymmetric Spindle Positioning Is Required for Cdc42 Activation

As Cdc42 activation only occurs at the spindle pole-cortex contact site (Ma et al., 2006), we wished to determine whether spindle pole-cortex contact was indeed required for Cdc42 activation. Earlier work by Gard (1992) has indicated that metaphase I spindle attachment to the oocyte cortex requires an intact cortical actin network. We have previously shown that expressing C3 ADP ribosyltransferase (Nemoto et al., 1991), a specific and potent Rho inhibitor, in GV oocytes disrupted cortical actin and caused metaphase I spindles to "sink" inside the oocyte cytoplasm (Ma et al., 2006). To bypass this phenotype and specifically explore the possibility of inhibiting spindle rotation (Gard, 1992), we injected C3 mRNA 60 min following GVBD when the metaphase I spindle had assembled near the oocyte surface (Gard, 1992). As shown in Figure 3A (and Movie S8), at the start of anaphase (00:20–00:22), the spindle remained parallel to the oocyte cortex. Interestingly, we also observed Aurora B localization between the separating chromosomes, consistent with spindle midzone association (arrows, 00:30). A short while after homolog separation, chromosomes recongressed and formed a single metaphase (II) spindle (we call this metaphase II because homolog separation had been completed earlier). Significantly, the active Cdc42 failed to rise above background (Figure 3B).

To determine whether we could further delay Rho inhibition to specifically inhibit cytokinesis (Bement et al., 2005; Ma et al., 2006) without affecting spindle rotation (Gard, 1992), we injected C3 mRNA at 90 min following GVBD. Approximately 30 min after C3 mRNA injection (or 2 hr after GVBD), anaphase initiated (Figure 3C, 00:04; evident by the thinning of microtubules in the middle of the spindle; also see Movie S9), and shortly after, active Cdc42 appeared at the spindle pole-cortex contact site (00:08, arrow). However, instead of developing a robust Cdc42 activity cap to enclose the extruding polar body (as is the case in control oocytes; see above), active Cdc42 was restricted to the same site for approximately 10 min before disappearing (00:18). These oocytes underwent complete chromosome separation (data not shown) but failed to extrude a polar body. Eventually, a single metaphase spindle emerged and became attached to the oocyte cortex (Figure 3C, 01:02). Thus, Cdc42 activation requires a bipolar metaphase I spindle with one pole attached to the oocyte cortex in a perpendicular configuration. However, because the level of Cdc42 activation never achieved what was seen in controls, the results also suggest that RhoA activity is required for full Cdc42 activation (also see below).

Ect2 in Polar Body Emission

To further investigate the functional interaction between Cdc42 and RhoA, we employed a dominant-negative mutant of *Xenopus* Ect2 (Tatsumoto et al., 2003). Ect2 has been implicated as a centralspindlin-associated RhoA GEF in controlling the cytokinetic contractile ring (Tatsumoto et al., 1999; Yuce et al., 2005), although what role, if any, this GEF plays in vertebrate polar body emission has not been described. Injection of DN-Ect2 inhibited polar body emission (87/94 failed, compared with 0/50 in control oocytes). As shown in Figure 4A, DN-Ect2 abolished formation of the ring-like RhoA activity zone, probed with eGFP-rGBD (rGBD: the Rho-binding domain of rhotekin, which binds only the GTP form of Rho [Benink and Bement, 2005]). DN-Ect2 did not affect spindle assembly, spindle-cortex contact, or homolog separation (Figure 4B and Movies S10 and S11). Interestingly, like C3 (Figure 3C), DN-Ect2 similarly diminished but did not eliminate Cdc42 activation (Figure 4C, DN-Ect2, and Movie S13). Similarly diminished Cdc42 activity was also observed in oocytes injected with Cdc42N17 (Figure 4C, Cdc42N17, and Movie S12), agreeing with our previous conclusion that that Cdc42N17 only partially inhibited Cdc42 (Benink and Bement, 2005; Ma et al., 2006).

To determine localization of Ect2 during polar body emission, we employed a GFP-tagged *Xenopus* Ect2 (Ect2-3GFP). Prior to anaphase initiation, very little specific Ect2 signal was detected (Figure 5A, 00:00, and Movies S14 and S15). At anaphase, Ect2 became clearly concentrated to a ring between the two spindle poles (00:01), reminiscent of central spindle-associated Aurora B (Figure 1D). In the next few minutes, the central spindle expanded laterally and attracted more Ect2. The ring started to constrict (00:09) and closed in less than 10 min (00:17). In oocytes injected with Cdc42N17, Ect2 also became concentrated at the central spindle, as in control oocytes. However, the Ect2 signal faded without contracting (Figure 5B and Movies S16 and S17; a total of 10 oocytes were imaged in three experiments and none contracted). Similarly, Ect2 signal was seen in oocytes

(B) Control oocytes and oocytes injected with ΔN cyclin B1 mRNA were treated with progesterone and fixed 3–4 hr after GVBD for chromosome analyses. Oocytes were scored as MII (metaphase II chromosome array and a polar body) or no polar body (PB). Shown are means (percentage of total oocytes examined, with SEM) of three independent experiments. The total numbers of oocytes in the three experiments are also included in the graph. Shown below are typical chromosome images of the two groups.

(C) A series from a 4D movie of a control oocyte (upper row) and an oocyte injected with ΔN cyclin B1 mRNA (lower row). These oocytes were also injected with rhodamine-tubulin (red) and eGFP-wGBD (active Cdc42, green). Note the complete lack of Cdc42 activation, and lack of a polar body (PB), in oocytes injected with ΔN cyclin B1 mRNA. Scale bar is 20 μm in all images of this paper. Time (hr:min) zero corresponds to the beginning of the time-lapse experiments, typically 100–120 min after GVBD. In some oocytes, the vitelline membrane (VM) is visible with the fluorescence probes.

(D) A series from a 4D movie of a control oocyte depicting dynamic localization of endogenous Aurora B (Alexa 488 anti-Aurora B, green) and microtubules (rhodamine-tubulin, red). Arrows indicate spindle midzone (MZ) or midbody (MB). Note that egg (MII) chromosomes (circle) appear much fainter (than polar body chromosomes) because they are obscured by the dense cytoplasm.

(E) A series from a 4D movie of an oocyte injected with ΔN cyclin B1 mRNA depicting endogenous Aurora B (Alexa 488 anti-Aur B, green) and microtubules (rhodamine-tubulin, red). Note the attachment of intact metaphase I spindle to the oocyte cortex for an extended period of time without chromosome separation.

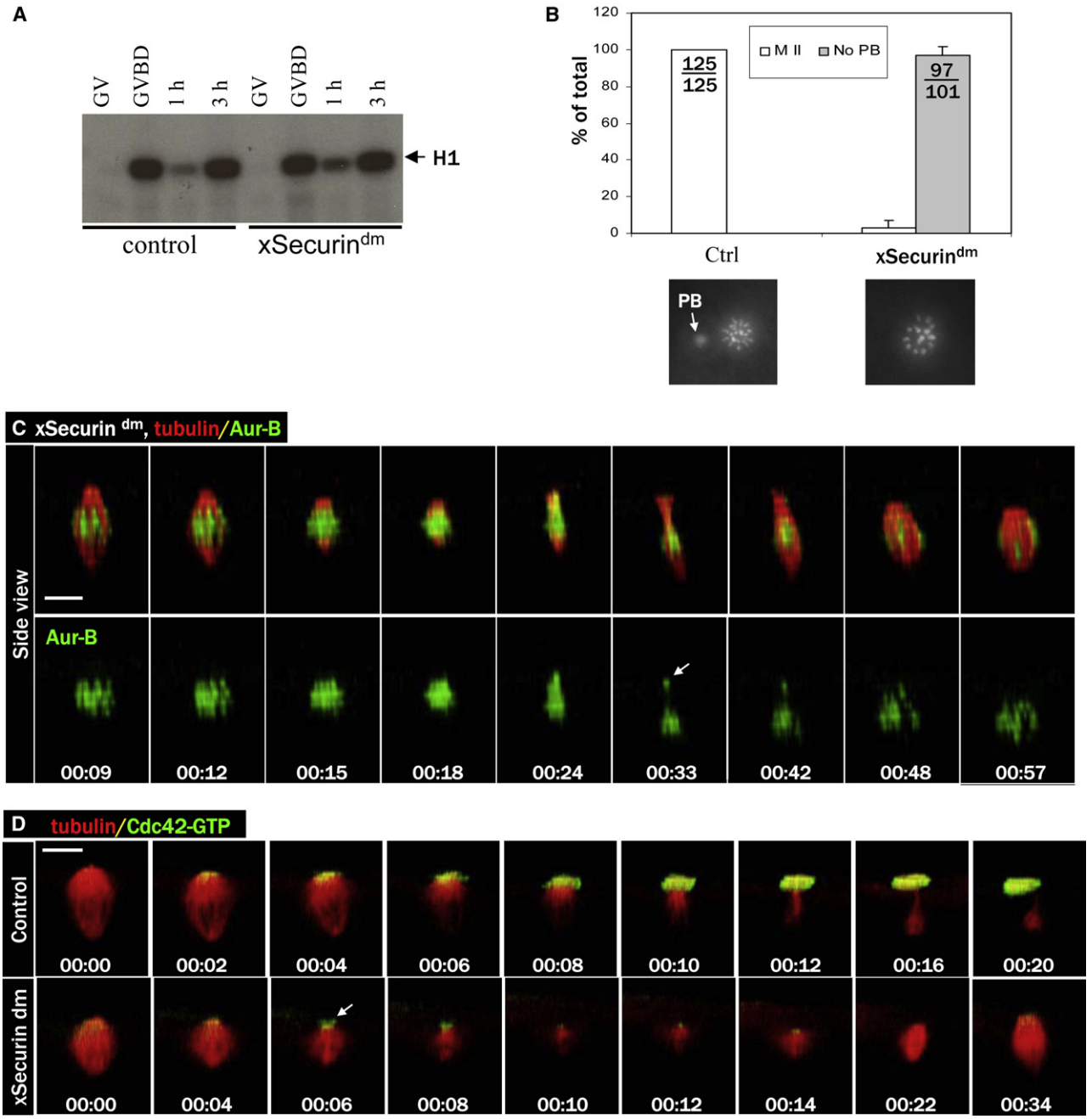

Figure 2. xSecurin^{dm} Inhibits Homolog Separation and Diminishes Cdc42 Activation

(A) Control oocytes and oocytes injected with xSecurin^{dm} mRNA were incubated with progesterone and withdrawn at the indicated time for MPF assays, as in Figure 1A.

(B) Control oocytes and oocytes injected with xSecurin^{dm} mRNA were treated with progesterone and fixed 3–4 h after GVBD for chromosome analyses, as in Figure 1B. Shown are means (percentage of total oocytes examined, with SEM) of three independent experiments.

(C) A series from a 4D movie of an oocyte injected with xSecurin^{dm} mRNA depicting endogenous Aurora B (Alexa 488 anti-Aur B, green) and microtubules (rhodamine-tubulin, red). Note the dramatic shortening of the spindle, without polar body emission.

(D) A series from a 4D movie of a control oocyte (upper row) and that of an oocyte injected with xSecurin^{dm} mRNA (lower row). These oocytes were also injected with rhodamine-tubulin (red) and eGFP-wGBD (active Cdc42, green). Cdc42 activation was diminished but not eliminated (arrow) in xSecurin dm-oocytes.

injected with xSecurin^{dm}, albeit often less intense and more disorganized than those in oocytes injected with Cdc42N17 (Figure 5C and Movies S18 and S19). In contrast, no specific Ect2 signal was seen in oocytes injected with ΔN cyclin B1 or methyl-Ub (data not shown). As expected, DN-Ect2 also completely eliminated any specific Ect2 signal (data not shown), as shown in mitosis (Chalamalasetty et al., 2006). These results indicate that the appearance of Ect2 signal at the central spindle is

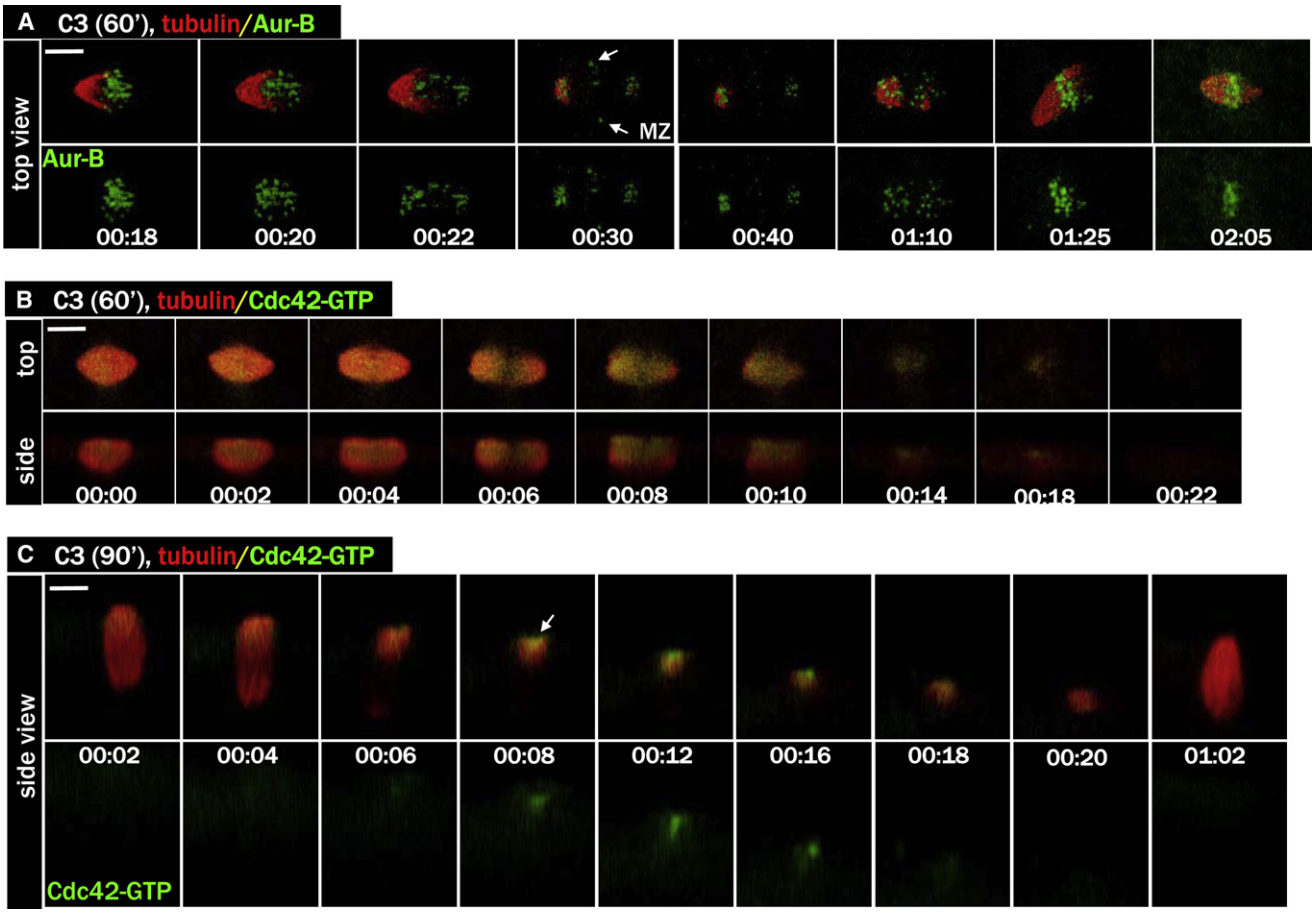

Figure 3. Cdc42 Activation Requires Spindle Pole Attachment to the Oocyte Cortex

(A) A series from a 4D movie of an oocyte injected with C3 mRNA 60 min following GVBD to inhibit spindle rotation (Alexa 488 anti-Aur B, green; rhodamine-tubulin, red). Note the complete separation of chromosome homologs with spindle midzone clearly visible (arrows, 00:30), and the subsequent recongressing of all chromosomes.

(B) A series from a 4D movie showing an oocyte injected with C3 mRNA 60 min after GVBD (eGFP-wGBD, green; rhodamine-tubulin, red). Note the complete absence of Cdc42 activation.

(C) A series from a 4D movie of an oocyte injected with C3 mRNA 90 min following GVBD (eGFP-wGBD, green; rhodamine-tubulin, red). Note the limited Cdc42 activation (arrow) that did not develop into a robust cap. No polar body formed.

associated with spindle changes during anaphase, and not with homolog separation per se.

Cdc42 Defines the Borders of RhoA Activity Zones by Inhibiting RhoA

The mutually exclusive zones of active Cdc42 and active RhoA during polar body formation (Ma et al., 2006) suggested that Cdc42 may somehow limit the boundaries of the RhoA zone, as described for single-cell wound healing in frog oocytes (Benink and Bement, 2005). To test this notion, we conducted time-lapse imaging in oocytes injected with Cdc42N17, together with probes for active Cdc42 (RFP-wGBD) and active RhoA (eGFP-rGBD). As shown previously (Ma et al., 2006), in control oocytes Cdc42 and RhoA formed complementary activity zones during polar body formation (Figure 6A and Movies S20–S22). In contrast, in oocytes injected with Cdc42N17, only residual Cdc42 activation was detected at the spindle pole-cortex contact site (data not shown, but see Figure 4C, bottom row). Remarkably, RhoA activity was very robust in these oocytes, with a higher overall level than that in control oocytes (Figure 6B and Movie S23). The organization of the RhoA zone was strikingly different than in controls: rather than forming a tight ring and closing rapidly, RhoA activity was spread out in much broader region, and, moreover, much of the active RhoA localized to discrete structures not seen in controls. Nonetheless, the RhoA activity zone still contracted and closed (Figure 6B; 7/15), although in other oocytes (8/15) the RhoA activity zone only partially contracted before subsiding (see Figure 7C).

Cdc42 Controls Actin Polymerization in the Cortex of the Protruding Polar Body

To better understand the roles of Cdc42 and RhoA in directing cytokinetic contractile ring formation and constriction, we carried out time-lapse imaging experiments using Alexa 594-G actin (to visualize dynamic actin polymerization [Burkel et al., 2007])

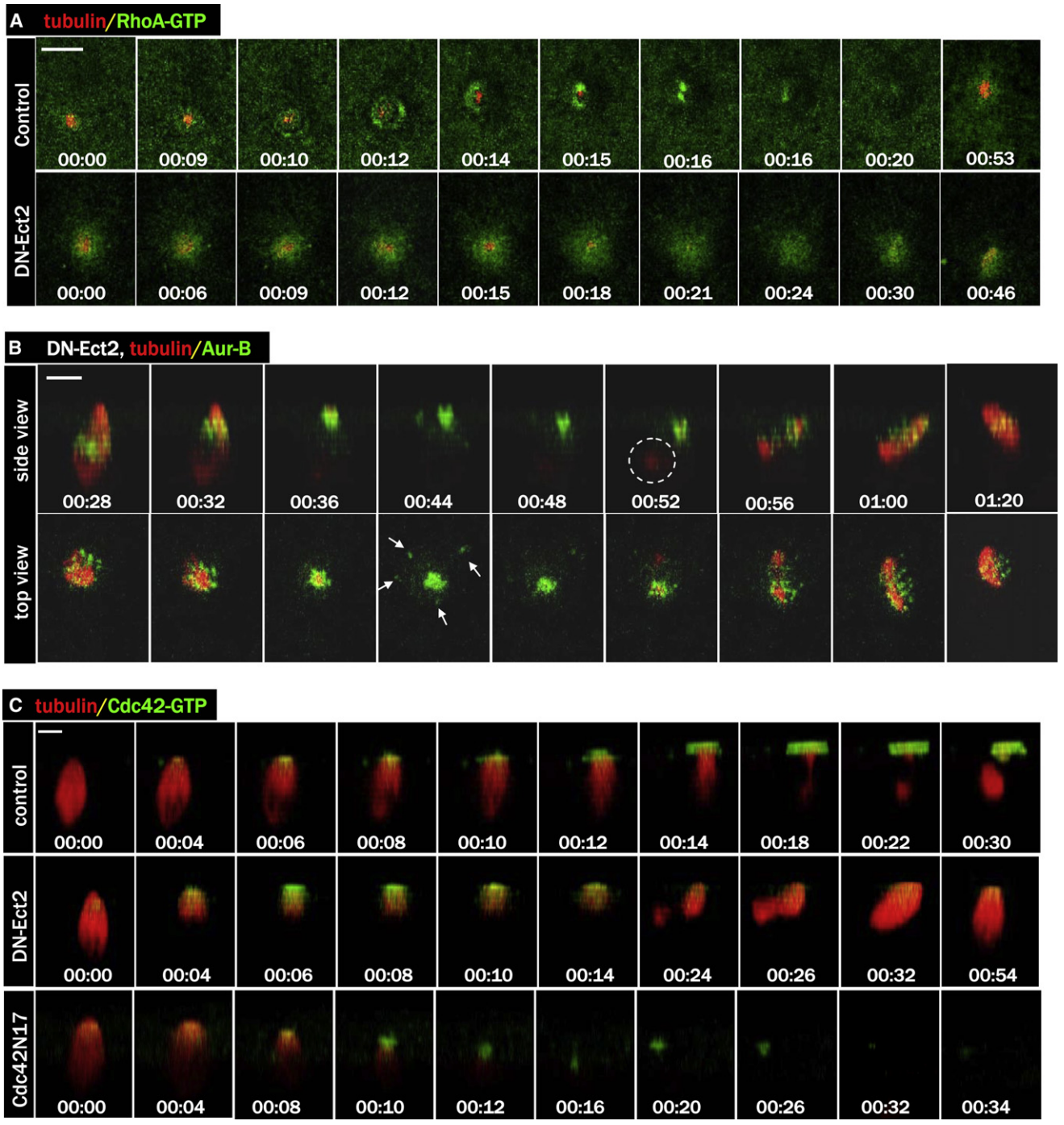

Figure 4. DN-Ect2 Inhibits RhoA Activity and Diminishes Cdc42 Activity

(A) A series from a 4D movie of a control oocyte (upper row) and that of an oocyte injected with DN-Ect2 mRNA (lower row). These oocytes were also injected with eGFP-rGBD (green) and rhodamine-tubulin (red). Note the absence of RhoA contractile ring in the DN-Ect2 oocyte.

(B) A series from a 4D movie of an oocyte injected with DN-Ect2 mRNA (Alexa 488 anti-Aur B, green; rhodamine-tubulin, red). Note the complete separation of chromosome homologs and the appearance of midzone Aurora B (arrows) before chromosome recongression. While the deeper chromosome set was difficult to see in some time points, the associated microtubule remnant was more evident (circle).

(C) A series from a 4D movie of a control oocyte (top row), that of an oocyte injected with DN-Ect2 mRNA (middle row), and that of an oocyte injected with Cdc42N17 mRNA (bottom row). These oocytes were also injected with eGFP-wGBD (green) and rhodamine-tubulin (red). Note that Cdc42 activation was diminished but not eliminated in oocytes injected with DN-Ect2 or Cdc42N17.

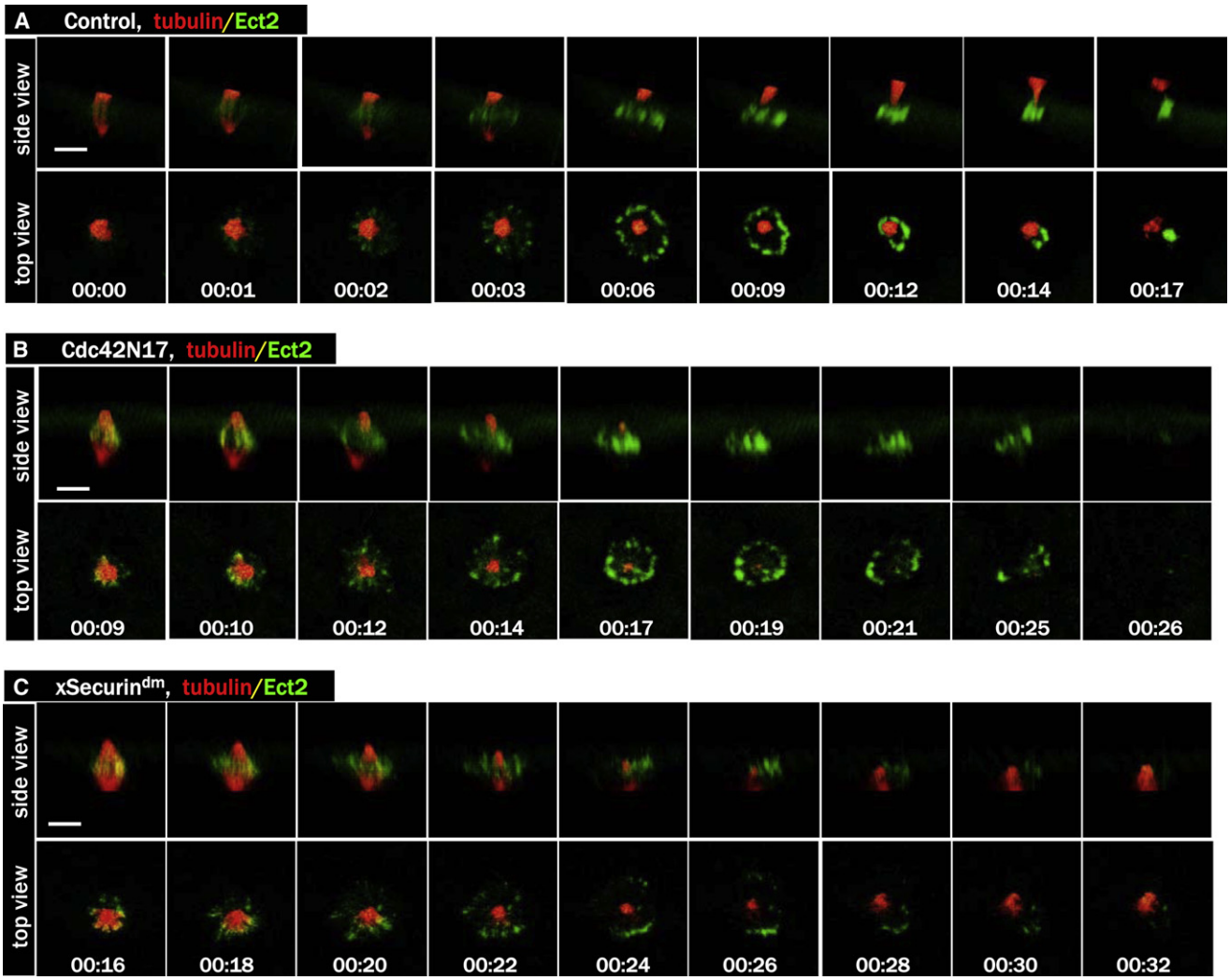

Figure 5. Dynamic Ect2 Localization during Polar Body Emission

(A) A series from a 4D movie of a control oocyte injected with rhodamine-tubulin (red) and Ect2-3GFP mRNA (green). Ect2 first appears at the central spindle and ends at the midbody.

(B) A series from a 4D movie of an oocyte injected with Cdc42N17 together with rhodamine-tubulin (red) and Ect2-3GFP (green). Ect2 appears at the central spindle but fades away without contraction.

(C) A series from a 4D movie of an oocyte injected with xSecurin^{dm} together with rhodamine-tubulin (red) and Ect2-3GFP (green). Ect2 signal appears more disorganized (than that in [B]) and similarly fades quickly.

together with the RhoA activity probe. Remarkably, the RhoA zone showed relatively little overlap with the dynamic actin, as the latter was largely confined to a cap over the forming polar body while the former remained a tight ring at the base of the forming polar body (Figure 7A and Movie S24). Because the pattern of dynamic actin closely resembled that of active Cdc42, the experiment was repeated using Alexa 594-G actin and active Cdc42 probe (eGFP-wGBD). Indeed, the distribution of active Cdc42 and dynamic actin showed almost complete overlap (Figure 7B), suggesting that Cdc42 is responsible for promoting the dynamic actin on the forming polar body surface. Consistent with this notion, the actin cap virtually disappeared in oocytes expressing Cdc42N17, while RhoA activity is very robust (Figure 7C and Movie S25).

RhoA Templates the Contractile Ring with Pre-existing/Formin-Nucleated F-Actin Filaments

The relative dearth of dynamic actin in the region of the RhoA zone suggested that RhoA and Cdc42 might play complementary roles during polar body emission, similar to their proposed role in cell wound repair, wherein the Cdc42 zone is responsible for directing formation of a region of relatively dynamic actin while RhoA is responsible for directing formation of a contractile ring comprising myosin-2 and stable actin (see Discussion). We therefore assessed the possibility that relatively stable and/or formin-nucleated F-actin concentrates in the RhoA zone. This was accomplished by microinjecting oocytes with fluorescent phalloidin, which, in contrast to fluorescent G-actin, can label relatively stable F-actin or F-actin nucleated by formins (Mandato

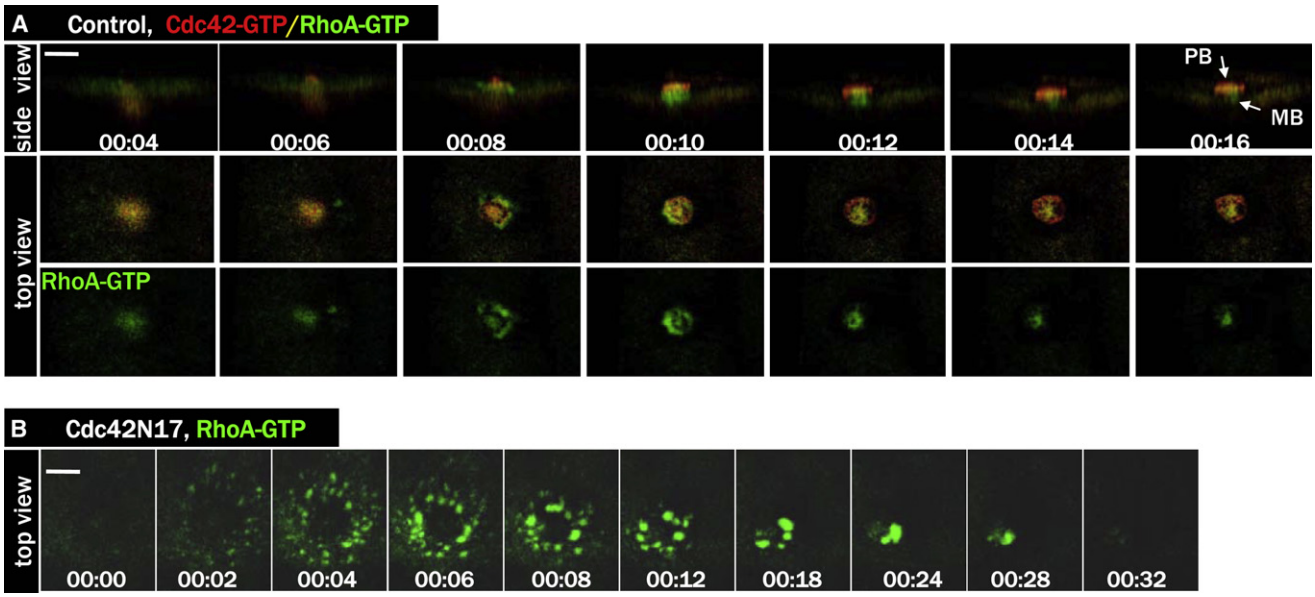

Figure 6. Inhibition of Cdc42 Caused Hyperactivation of RhoA

(A) A series from a 4D movie of a control oocyte exhibiting dynamic and complementary activity zones of RhoA (eGFP-rGBD, green) and Cdc42 (RFP-wGBD, red) during polar body (PB) formation. MB, midbody.

(B) A series from a 4D movie of a Cdc42N17-injected oocyte with the same two probes as in (A). Only eGFP-rGBD signal was shown. Note that the RhoA activity zone spreads out in much larger area.

and Bement, 2003; Burkel et al., 2007). In contrast to the fluorescent G-actin, fluorescent phalloidin showed considerable overlap with the constricting RhoA zone (arrows) as well as the surface of the forming polar body (Figure 7D and Movies S26 and S27), indicating that the RhoA zone controls a pool of F-actin during polar body emission that differs from that controlled by Cdc42. In addition, the RhoA-based contractile ring also contained phosphorylated (active) myosin light chain (pMLC, Figures S2A and S2B), indicating that RhoA templated a classical actomyosin contractile ring during polar body emission. In Cdc42N17 oocytes, very little F-actin signal was observed, either with G-actin probe (Figure 7C) or with phalloidin probe (Ma et al., 2006), despite prominent RhoA activity and associated pMLC (Figures S2C and S2D). These results suggest the Cdc42 zone somehow influences the supply of F-actin for the RhoA-based contractile ring.

Cdc42 Controls Polar Body Outpocketing

The above results suggested that during polar body emission, RhoA templates formation of a classic contractile ring, while Cdc42 somehow abets this process by templating formation of a cap of highly dynamic actin. To assess the mechanistic contributions of the latter structure to polar body emission, the effects of Cdc42 inhibition were monitored in more detail by following the distribution of both chromosomes and the RhoA activity zone. In control oocytes, constriction of the RhoA zone occurs coincident with protrusion of the polar body chromosomes (Figure 8A, top row, and Movie S29) and outpocketing of the plasma membrane (Figure S3), resulting in excision of the polar body. In contrast, when Cdc42 is inhibited, the RhoA zone undergoes a futile, and often partial, constriction, closing over a flat plasma membrane and trapping both sets of chromosomes in the eggs (Figure 8A, middle row, and Movie S28), which eventually recongress into a single metaphase spindle (Ma et al., 2006). Similar but less organized RhoA activity zone was also observed in oocytes injected with xSecurin^{dm}, despite the lack of homolog separation (Figure 8A, bottom row, and Movie S30).

To further investigate the relationship between the RhoA contractile ring and the dynamic Ect2 ring, we employed RFP-Ect2 together with eGFP-rGBD for double imaging. A distinct Ect2 ring could be seen (Figure 8B, 00:02, and Movies S31 and S32) several minutes before the RhoA contractile ring became evident (00:08). Surprisingly, the two rings never overlapped. The RhoA ring appeared at the level of the plasma membrane and appeared to constrict and close at the plasma membrane. In contrast, the Ect2 ring first appeared approximately 20 μm below the levels of the plasma membrane (00:02, arrow), consistent with its spindle (approximately 40 μm in length) midzone position at this point (before polar body outpocking). As the Ect2 ring constricted, it also progressively moved up toward the plasma membrane until it reached the constricting RhoA ring at the midbody (00:14). At the midbody, it could be seen that the Ect2 signal formed the core, wrapped around by the active RhoA ring (inset, top right).

DISCUSSION

Coupling of the final step of cell division to proper spindle orientation is an event particularly important for vertebrate female meiosis. We previously showed that local Cdc42 activation at the site of spindle pole-plasma membrane contact is an essential part of this coupling (Ma et al., 2006). Here we have identified several distinct, but possibly linked, inputs that are needed for proper Cdc42 activation: spindle rotation, anaphase initiation, and RhoA activation.

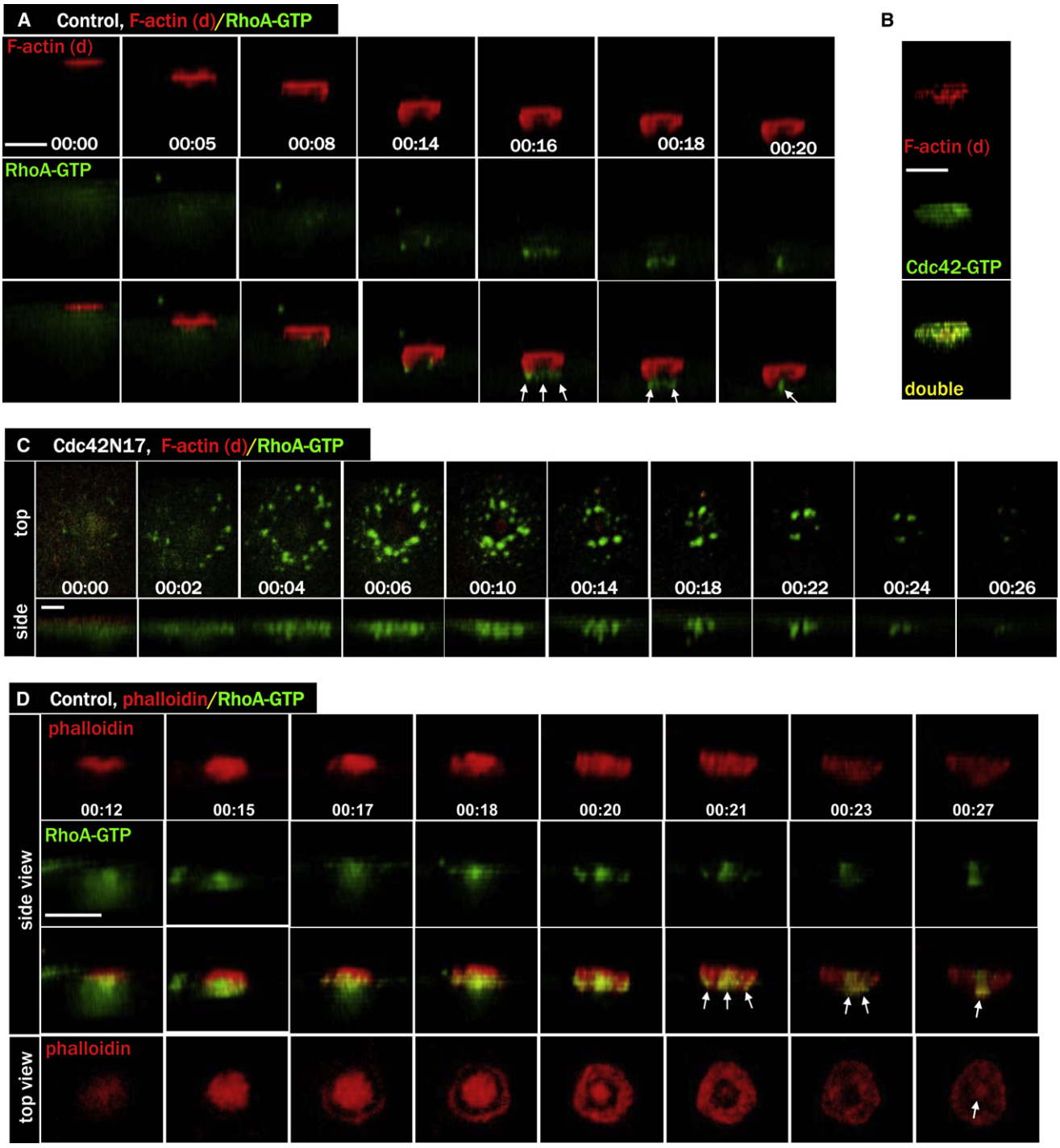

Figure 7. Cdc42 Templates a Dynamic F-Actin Cap Corresponding to the Forming Polar Body

(A) Side view of a series from a 4D movie of a control oocyte exhibiting dynamic (d) F-actin signal (Alexa 594-G actin, red) and RhoA activity (eGFP-rGBD, green). The RhoA contractile ring had very little dynamic F-actin.

(B) A single time point depicting the complete overlap between dynamic (d) F-actin (Alexa 594 G actin, red) and Cdc42 activity (eGFP-wGBD, green) during polar body emission.

(C) A series from a 4D movie of a Cdc42N17-injected oocyte, with the same two probes as in (A), indicating the lack of a robust dynamic actin cap. Only residual F-actin signal was detected at the center of the robust RhoA zone, coinciding with the residual Cdc42 activity (Figure 4C, bottom row).

(D) A series from a 4D movie of an oocyte exhibiting both dynamic and stable F-actin (Alexa 594 phalloidin, red) and RhoA activity (eGFP-rGBD, green). Note the significant overlap of the phalloidin probe with the RhoA contractile ring (arrows). The F-actin signal in the "roof" of the polar body (00:15, bottom row) progressively thins out during latter stage of polar body emission so the top is open, exposing the phalloidin-labeled midbody (arrow, 00:27).

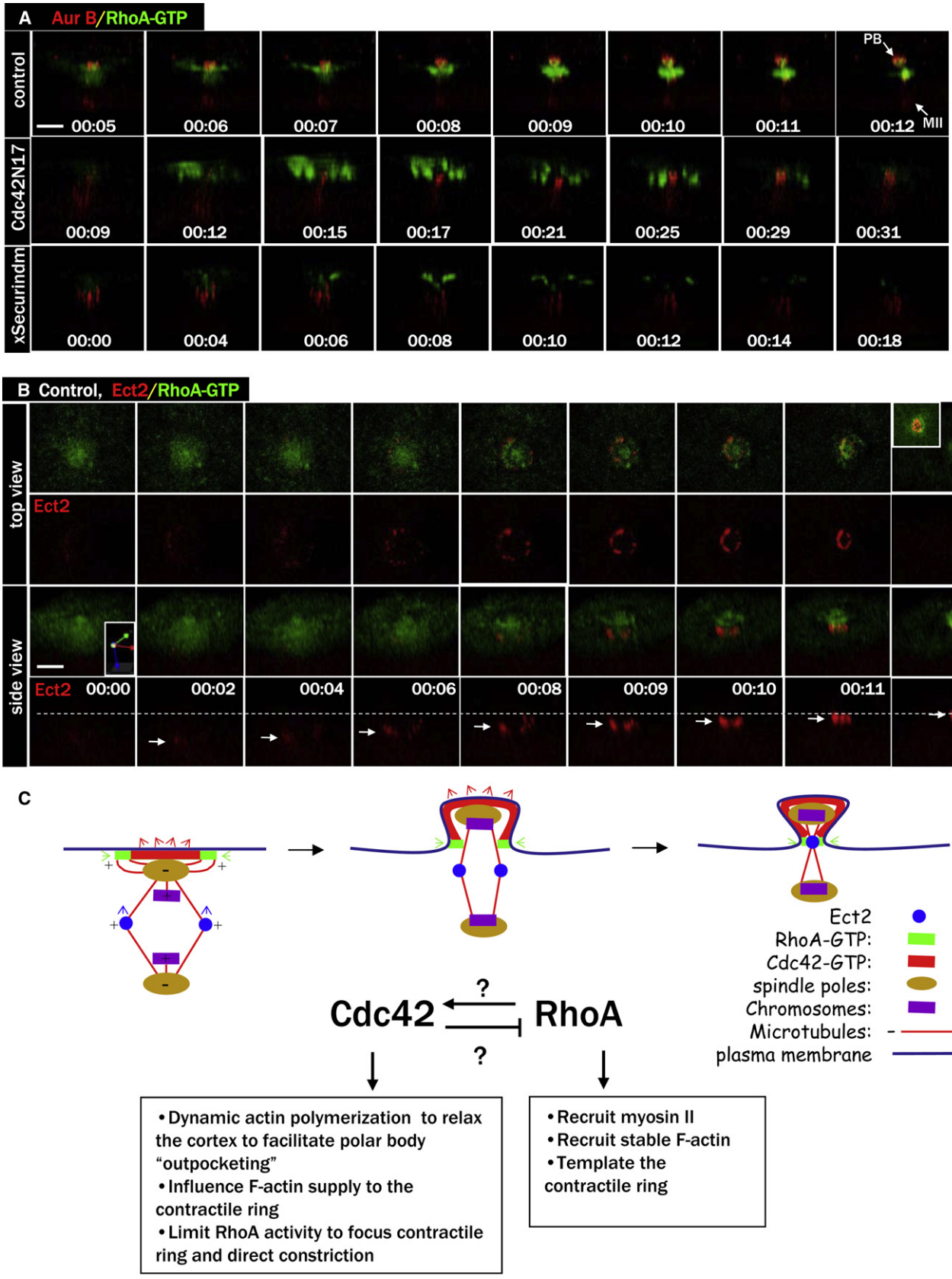
A Aur B/RhoA-GTP
control
Cdc42N17
xSecurindm
PB
MII
00:05
00:06
00:07
00:08
00:09
00:10
00:11
00:12
00:09
00:12
00:15
00:17
00:21
00:25
00:29
00:31
00:00
00:04
00:06
00:08
00:10
00:12
00:14
00:18
B Control, Ect2/RhoA-GTP
top view
Ect2
side view
Ect2 00:00
00:02
00:04
00:06
00:08
00:09
00:10
00:11
00:14
C
Ect2
RhoA-GTP:
Cdc42-GTP:
spindle poles:
Chromosomes:
Microtubules:
plasma membrane
Cdc42
?
?
RhoA
• Dynamic actin polymerization to relax the cortex to facilitate polar body "outpocketing"
• Influence F-actin supply to the contractile ring
• Limit RhoA activity to focus contractile ring and direct constriction
• Recruit myosin II
• Recruit stable F-actin
• Template the contractile ring

While the first of these inputs, anaphase initiation, might seem like an obvious requirement, in fact this question has been attended by considerable controversy. That is, it has previously been reported that homolog separation and polar body emission in frog oocytes represents an anomaly in not requiring polyubiquitination-mediated proteolysis (Taieb et al., 2001; Peter et al., 2001), in contrast to not only homolog separation and polar body emission in mouse oocytes (Herbert et al., 2003; Kudo et al., 2006; Terret et al., 2003) but in meiosis of all other organisms including yeast (Kudo et al., 2006, and references therein). Based on experiments employing three different approaches, we find that homolog separation in frog oocytes is no exception in requiring polyubiquitination-mediated proteolysis. More importantly for this study, Cdc42 activation and polar body emission are likewise dependent on proteolysis-dependent inactivation of Cdk1 and resultant anaphase initiation. It is not clear why our results differ from previous studies (Taieb et al., 2001; Peter et al., 2001), and in particular those of Peter et al. (2001), who not only monitored polar body emission per se but also employed some of the same approaches used here. It is possible that in oocytes injected with the D box peptide, overall cyclin B degradation was inhibited but at the site of the spindles there was sufficient cyclin B degradation (and MPF inactivation) to permit anaphase (Peter et al., 2001). In contrast, ΔN cyclin B1 derived from mRNA injection (in this study) may better maintain MPF activity near the spindle to inhibit anaphase since localized translation of cyclin mRNA on spindles has been previously described (Groisman et al., 2000). Similarly, we found that anaphase inhibition by methylubiquitin was dose sensitive, requiring at least 500 ng (Boston Biotech) per oocyte. As Peter et al. (2001) employed a different source of methylubiquitin, it is difficult to compare the potency in the two studies. On the other hand, our results are consistent with those of Gorr et al. (2006), who found that polar body emission in both frog and mouse oocytes was prevented when Cdk1 inactivation was blocked, but could be subsequently rescued via pharmacological inhibition of Cdk1.

Whereas multiple factors affect Cdc42 activation, the most critical among them appears to be spindle pole-cortex contact and anaphase initiation. Specifically, no Cdc42 activation was observed in oocytes that underwent anaphase while metaphase I spindles lay parallel to the oocyte cortex (Figure 3B), or in oocytes in which anaphase initiation was inhibited by ΔN cyclin B1 (Figure 1C) or methylubiquitin (Figure S1C). Although the transient inactivation of Cdk1 is required for Cdc42 activation, it is unlikely the direct trigger. In frog oocytes, degradation of cyclin B occurs shortly after GVBD, and MPF activity reaches the lowest levels by 60 min after GVBD (Figures 1A and 2A and Figure S1A), more than an hour before Cdc42 activation is observed. On the other hand, Cdc42 activation is always coupled temporally (within a few minutes) to anaphase initiation, suggesting that anaphase functions as a trigger for Cdc42 activation. Specifically, Cdc42 activation is coupled to anaphase-specific spindle changes (kinetochore microtubule shortening and central spindle formation), rather than homolog separation per se (see Figure 2D). However, full Cdc42 activation and cytokinesis eventually failed in the absence of homolog separation (in oocytes injected with xSecurin^{dm}), reminiscent of the failed cytokinesis induced by inhibition of Cdk1 in the absence of chromosome separation during mitosis (Niiya et al., 2005). The dual determinants (asymmetric spindle pole attachment to the oocyte cortex and anaphase initiation) thus provide the temporal and spatial cues for Cdc42 activation, and hence for this unique form of cytokinesis. In addition, full activation of Cdc42 also requires concomitant RhoA activation; the latter patterns the contractile ring. Without RhoA activation, the Cdc42 activity zone is restricted to the initial spindle pole-cortex contact site. Exactly how RhoA activity influences Cdc42 activity is not known. It may be achieved through a direct mechanism in which the dynamic RhoA activity zone helps sustain the expanding and complementary Cdc42 activity zone, or indirectly though the formation of the nascent structure (forming polar body) in which Cdc42 activity can grow.

Although Ect2 has been implicated as a GEF for RhoA during mitotic cytokinesis (Tatsumoto et al., 1999; Yuce et al., 2005), our data demonstrate the dynamic association of Ect2 with the cytokinetic structures (central spindles and midbody) in live cells. Notwithstanding the possibility that our GFP-tagged (and RFP-tagged) Ect2 does not accurately reflect the natural localization of endogenous Ect2, our data clearly indicated that Ect2 never overlapped with the active RhoA zone in the oocytes, and therefore Ect2 is unlikely a direct activator (GEF) of RhoA during polar body emission. Interestingly, a recent study (Birkenfeld et al., 2007) has identified GEF-H1 as the direct GEF to activate Rho during cytokinesis in HeLa cells. We propose (Figure 8C) that shortly after anaphase initiation, the spindle pole (microtubule minus end)-directed activation of Cdc42 is coordinated by the almost simultaneous activation of RhoA, possibly by microtubule

Figure 8. RhoA Contracts Nonproductively in Cdc42N17 Oocytes

(A) Top row: Side view of a series from a 4D movie of a control oocyte injected with Alexa 594-anti-Aur B and eGFP-rGBD. Note that the RhoA contractile ring constricted between the two sets of chromosomes to complete polar body (PB) emission. Middle row: Side view of a series from a 4D movie of an oocyte injected with Cdc42N17 mRNA, together with the same two probes. RhoA constricted partially, over both sets of chromosomes, resulting in failure of cytokinesis. Bottom row: Side view of a series from a 4D movie of an oocyte injected with xSecurin^{dm} mRNA, together with the same two probes. The RhoA signal appeared disorganized over the unseparated chromosomes before fading away.

(B) A series from a 4D movie of an oocyte injected with RFP-Ect2 (red) together with the Rho activity probe eGFP-rGBD (green). The Ect2 ring never overlaps with the Rho contractile ring. The inset (top right) depicts an interior view of the core Ect2 ring wrapped around by the RhoA contractile ring at this time point. The dashed line marks the level of the plasma membrane (and RhoA contractile ring), and arrows indicate the levels of the Ect2 ring. The side view of this series is slightly tilted (see xyz coordinates) to show the relatively weak RFP-Ect2 signal at earlier time points.

(C) A working model depicting the differential roles and regulation of Cdc42 and RhoA during female meiotic cytokinesis (side view). Cdc42 and RhoA may be activated by GEFs associated with the spindle pole (microtubule minus ends) and microtubule tips (plus ends), respectively. Cdc42 and RhoA may also functionally regulate each other (explained in the text). While the contractile ring (active RhoA and myosin II) has intrinsic contractility independent of Cdc42 function (see Figure 6B), the apparent constriction of the Ect2 ring (central spindles) is the result of Cdc42-controlled plasma membrane outpocketing, pulling the spindle upward through the constricting contractile ring.

tip (plus end)-associated GEF (e.g., GEF-H1). The striking RhoA activity dots in oocytes injected with Cdc42N17 (e.g., Figure 6B) would support this hypothesis. The differential activation of RhoA and Cdc42 by microtubules, together with a possible direct inhibition of RhoA by Cdc42, could explain the complementary and mutually exclusive temporal relationship of RhoA and Cdc42 activity zones during polar body emission. During contractile ring constriction, the role of Cdc42 appears to facilitate plasma membrane outpocketing (see Figure S3), pulling the spindle upward through the constricting RhoA contractile ring (hence the concomitant Ect2 ring constriction) until the central spindle reaches the constricted contractile ring (Figure 8C). In oocytes injected with Cdc42N17, the RhoA/myosin II contractile ring constricts, often partially. However, without the upward pulling of Cdc42, the RhoA constriction is futile and never accompanied by Ect2 ring constriction (Figure 5B). Although Ect2 does not appear to colocalize with active RhoA during cytokinesis, it is clearly required for RhoA contractile ring formation during polar body emission (Figure 4A), as is in mitosis (Tatsumoto et al., 1999; Yuce et al., 2005). In addition, it is also required for proper Cdc42 activation (Figure 4C), possibly indirectly through RhoA. Precisely how Ect2 regulates the contractile ring and its constriction remains unsolved here and, in our opinion, in mitosis as well.

The striking overlap of the Cdc42 zone with dynamic F-actin (Figure 7B) indicated that Cdc42 promotes rapid actin polymerization over the cortex of the protruding polar body. Our analysis suggests that Cdc42 activity and the highly dynamic actin polymerization it promotes are required for the outpocketing of the plasma membrane. We therefore propose that Cdc42 and the highly dynamic actin serve to relax the cortex of the protruding polar body. Such relaxation could be achieved by either Cdc42-dependent suppression of myosin-2 activity (Mandato et al., 2000) or if the dynamic F-actin is a relatively poor substrate for myosin-2 or other crosslinkers by virtue of its short half-life.

Regardless of exactly how Cdc42 contributes to outpocketing, the results clearly indicate that RhoA and Cdc42 control distinct but complementary aspects of the cytoskeletal function during polar body emission. That is, the RhoA zone directs local formation of a classic contractile ring composed of myosin-2 and relatively stable F-actin and/or F-actin polymerized via formins, while the Cdc42 zone directs formation of a spatially distinct region rich in highly dynamic actin and virtually devoid of myosin-2. The actomyosin ring, in turn, powers constriction of the contractile apparatus with the associated plasma membrane, while the Cdc42 zone promotes outward pocketing of the plasma membrane to enclose the polar body chromosomes. These findings are fascinating not only in that they help explain how this highly asymmetric cell division is accomplished but also from the point of view of their similarity to what might otherwise be considered a completely different process, namely, repair of the *Xenopus* oocyte cortical cytoskeleton following cell damage (Benink and Bement, 2005). In that system, Rho and Cdc42 are also activated in complementary zones, but with the opposite organization, such that the Rho zone is circumscribed by the Cdc42 zone. Further, as in polar body emission, the Cdc42 zone in wound repair directs formation of a region of highly dynamic F-actin, while the Rho zone directs formation of a contractile ring rich in relatively stable F-actin and myosin-2. These observations support the notion that Rho GTPase activity zones represent conserved signaling mechanisms that are harnessed to regulate diverse actomyosin-dependent events (Bement et al., 2006).

This study provides a mechanistic explanation to the question of how Cdc42 and RhoA work together to accomplish cytokinesis. Although polar body emission is a unique form of asymmetric cell division, it is intriguing to speculate that principles described in this paper may have wider implications in asymmetric cell division of other systems.

EXPERIMENTAL PROCEDURES

Plasmid DNA Construction and mRNA Synthesis

The dominant-negative mutant of Cdc42 ($Cdc42^{T17N}$) and Myc-tagged Botulinum C3 toxin have been described previously (Ma et al., 2006). GFP-Utr-CH, eGFP-wGBD, RFP-wGBD, and eGFP-rGBD constructs have been described previously (Sokac et al., 2003; Burkel et al., 2007). Full-length *Xenopus* Ect2 cDNA was a gift from Dr. T. Miki and was inserted into pCS2-C 3GFP or pCS2-mRFP, resulting in Ect2-3GFP (three copies of eGFP at the C terminus) or RFP-Ect2, respectively. Dominant-negative *Xenopus* Ect2 (amino acids 1–390) was PCR-amplified and inserted into pCS2 vector. The sequence of $Securin^{dm}$ (Zou et al., 1999) was PCR-amplified and subcloned into pCS2+HA (Booth et al., 2002). The destruction box mutant of cyclin B1 plasmid (ΔN cyclin B1) (Gross et al., 2001) was a gift from Dr. James Maller. All cDNA constructs were linearized before in vitro transcription using Ambion's mMESSAGE kit (5′ capped). mRNAs were dissolved in water to 1 mg per ml. Typically, 10 nl was injected per oocyte, although mRNAs coding for fluorescent probes often required concentration calibration for optimum fluorescence quality. C3 mRNA (Ma et al., 2006) was further diluted to 20 μg/ml in water, and 10 nl was injected per oocyte at the indicated time following GVBD. Additional information on chemicals, antibodies, fluorescent probes, and conjugation of antibodies to Alexa fluorophores is in the Supplemental Data.

Time-Lapse Confocal Fluorescence Imaging of *Xenopus* Oocytes

Oocytes were typically injected with mRNA and fluorephorescence probes the day before imaging experiments and incubated overnight in OR2 at 20°C. The injected oocytes were placed in OR2 containing 1 μM progesterone in the morning and monitored for GVBD (the appearance of the white maturation spot). Occasionally, we would add progesterone the night of the injection (with at least 6 hr between mRNA injection and the addition of progesterone), in which case we would place the oocytes at 16°C following the addition of progesterone. Oocytes were transferred to 20°C in the morning and monitored for GVBD. This maneuver (16°C overnight) often saved hours in the morning before the first oocyte to appear GVBD. GVBD oocytes were individually transferred to fresh OR2 and further incubated until imaging time. Although individual oocytes vary, often considerably, in the timing of GVBD following the addition of progesterone, we found that they are remarkably synchronized from the first appearance of the GVBD spot to first polar body emission (Ma et al., 2006). Typically, 120 min after the first appearance of GVBD, the oocyte initiates anaphase I, evident by kinetochore microtubule shortening or chromosome separation (depending on the probes used). Within a few minutes, cytokinesis starts, evident by the activation of Cdc42 and RhoA (contractile ring). The constriction of the contractile ring takes less than 10 min, so we typically started imaging 100–120 min after the appearance of the GVBD spot. Time zero (00:00) corresponds to the start of the imaging experiments. Oocytes were imaged with a 60× oil objective on a Zeiss Axiovert with a BioRad 1024 laser scanning confocal imaging system. Time-lapse image series (Bement et al., 2003) were collected at various time intervals (30 s to 5 min depending on the experiments). Each time point volume comprised 15–30 image planes 1–3 μm apart. Image series were 3D-rendered using Volocity Presentation Software (Improvision). Some movies were made by combining more than one image sequence derived from the same oocyte, necessitated by the need to refocus during time-lapse experiments. Snapshots were taken at the indicated time points, either top view or side view, of these 3D series. Each of these imaging experiments was performed

at least three times, each with a different frog on a different day, with multiple oocytes being imaged on the same day.

SUPPLEMENTAL DATA

Supplemental data include additional Supplemental Experimental Procedures, 3 figures, and 32 movies. The movies are titled according to the corresponding figures shown in the paper. They can be found with this article online at http://www.developmentalcell.com/cgi/content/full/15/3/386/DC1/.

ACKNOWLEDGMENTS

We thank the following colleagues for reagents: Dr. James Maller (ΔN cyclin B1 cDNA and antibodies against cyclin B), Dr. Hui Zou (xSecurin^{dm} cDNA), Dr. Marie-Helene Verlhac (pRN3-β5-tubulin-GFP cDNA), and Dr. T. Miki (*Xenopus* Ect2 plasmid). This work is supported by operating grants from the National Cancer Institute of Canada and the Canadian Institute of Health Research (to X.J.L.), NIH GM52932 (to W.M.B.), and a Helen Hay Whitney fellowship (to A.L.M.).

Received: April 8, 2008
Revised: June 18, 2008
Accepted: July 15, 2008
Published: September 15, 2008

REFERENCES

Bement, W.M., Sokac, A.M., and Mandato, C.A. (2003). Four-dimensional imaging of cytoskeletal dynamics in Xenopus oocytes and eggs. Differentiation *71*, 518–527.

Bement, W.M., Benink, H.A., and von Dassow, G. (2005). A microtubule-dependent zone of active RhoA during cleavage plane specification. J. Cell Biol. *170*, 91–101.

Bement, W.M., Miller, A.L., and von Dassow, G. (2006). Rho GTPase activity zones and transient contractile arrays. Bioessays *28*, 983–993.

Benink, H.A., and Bement, W.M. (2005). Concentric zones of active RhoA and Cdc42 around single cell wounds. J. Cell Biol. *168*, 429–439.

Birkenfeld, J., Nalbant, P., Bohl, B.P., Pertz, O., Hahn, K.M., and Bokoch, G.M. (2007). GEF-H1 modulates localized RhoA activation during cytokinesis under the control of mitotic kinases. Dev. Cell *12*, 699–712.

Booth, R.A., Cummings, C., Tiberi, M., and Liu, X.J. (2002). GIPC participates in G protein signaling downstream of IGF-1 receptor. J. Biol. Chem. *277*, 6719–6725.

Burkel, B.M., von Dassow, G., and Bement, W.M. (2007). Versatile fluorescent probes for actin filaments based on the actin-binding domain of utrophin. Cell Motil. Cytoskeleton *64*, 822–832.

Chalamalasetty, R.B., Hummer, S., Nigg, E.A., and Sillje, H.H. (2006). Influence of human Ect2 depletion and overexpression on cleavage furrow formation and abscission. J. Cell Sci. *119*, 3008–3019.

Gard, D.L. (1992). Microtubule organization during maturation of Xenopus oocytes: assembly and rotation of the meiotic spindle. Dev. Biol. *151*, 516–530.

Gautier, J., Minshull, J., Lohka, M., Glotzer, M., Hunt, T., and Maller, J.L. (1990). Cyclin is a component of maturation-promoting factor from *Xenopus*. Cell *60*, 487–494.

Gerhart, J., Wu, M., and Kirschner, M. (1984). Cell cycle dynamics of an M-phase-specific cytoplasmic factor in Xenopus laevis oocytes and eggs. J. Cell Biol. *98*, 1247–1255.

Gorr, I.H., Reis, A., Boos, D., Wuhr, M., Madgwick, S., Jones, K.T., and Stemmann, O. (2006). Essential CDK1-inhibitory role for separase during meiosis I in vertebrate oocytes. Nat. Cell Biol. *8*, 1035–1037.

Groisman, I., Huang, Y.S., Mendez, R., Cao, Q., Theurkauf, W., and Richter, J.D. (2000). CPEB, maskin, and cyclin B1 mRNA at the mitotic apparatus: implications for local translational control of cell division. Cell *103*, 435–447.

Gross, S.D., Schwab, M.S., Taieb, F.E., Lewellyn, A.L., Qian, Y.W., and Maller, J.L. (2000). The critical role of the MAP kinase pathway in meiosis II in *Xenopus* oocytes is mediated by p90(Rsk). Curr. Biol. *10*, 430–438.

Gross, S.D., Lewellyn, A.L., and Maller, J.L. (2001). A constitutively active form of the protein kinase p90Rsk1 is sufficient to trigger the G2/M transition in Xenopus oocytes. J. Biol. Chem. *276*, 46099–46103.

Herbert, M., Levasseur, M., Homer, H., Yallop, K., Murdoch, A., and McDougall, A. (2003). Homologue disjunction in mouse oocytes requires proteolysis of securin and cyclin B1. Nat. Cell Biol. *5*, 1023–1025.

Hochegger, H., Klotzbucher, A., Kirk, J., Howell, M., Le Guellec, K., Fletcher, K., Duncan, T., Sohail, M., and Hunt, T. (2001). New B-type cyclin synthesis is required between meiosis I and II during Xenopus oocyte maturation. Development *128*, 3795–3807.

Iwabuchi, M., Ohsumi, K., Yamamoto, T.M., Sawada, W., and Kishimoto, T. (2000). Residual Cdc2 activity remaining at meiosis I exit is essential for meiotic M-M transition in Xenopus oocyte extracts. EMBO J. *19*, 4513–4523.

Kudo, N.R., Wassmann, K., Anger, M., Schuh, M., Wirth, K.G., Xu, H., Helmhart, W., Kudo, H., McKay, M., Maro, B., et al. (2006). Resolution of chiasmata in oocytes requires separase-mediated proteolysis. Cell *126*, 135–146.

Ma, C., Cummings, C., and Liu, X.J. (2003). Biphasic activation of Aurora-A kinase during the meiosis I- meiosis II transition in Xenopus oocytes. Mol. Cell. Biol. *23*, 1703–1716.

Ma, C., Benink, H.A., Cheng, D., Montplaisir, V., Wang, L., Xi, Y., Zheng, P.P., Bement, W.M., and Liu, X.J. (2006). Cdc42 activation couples spindle positioning to first polar body formation in oocyte maturation. Curr. Biol. *16*, 214–220.

Mandato, C.A., and Bement, W.M. (2003). Actomyosin transports microtubules and microtubules control actomyosin recruitment during *Xenopus* oocyte wound healing. Curr. Biol. *13*, 1096–1105.

Mandato, C.A., Benink, H.A., and Bement, W.M. (2000). Microtubule-actomyosin interactions in cortical flow and cytokinesis. Cell Motil. Cytoskeleton *45*, 87–92.

Maro, B., and Verlhac, M.H. (2002). Polar body formation: new rules for asymmetric divisions. Nat. Cell Biol. *4*, E281–E283.

Masui, Y., and Markert, C.L. (1971). Cytoplasmic control of nuclear behavior during meiotic maturation of frog oocytes. J. Exp. Zool. *177*, 129–146.

Mendez, R., Barnard, D., and Richter, J.D. (2002). Differential mRNA translation and meiotic progression require Cdc2-mediated CPEB destruction. EMBO J. *21*, 1833–1844.

Nemoto, Y., Namba, T., Kozaki, S., and Narumiya, S. (1991). Clostridium botulinum C3 ADP-ribosyltransferase gene. Cloning, sequencing, and expression of a functional protein in Escherichia coli. J. Biol. Chem. *266*, 19312–19319.

Niiya, F., Xie, X., Lee, K.S., Inoue, H., and Miki, T. (2005). Inhibition of cyclin-dependent kinase 1 induces cytokinesis without chromosome segregation in an ECT2 and MgcRacGAP-dependent manner. J. Biol. Chem. *280*, 36502–36509.

Peter, M., Castro, A., Lorca, T., Le Peuch, C., Magnaghi-Jaulin, L., Doree, M., and Labbe, J.C. (2001). The APC is dispensable for first meiotic anaphase in Xenopus oocytes. Nat. Cell Biol. *3*, 83–87.

Rogers, E., Bishop, J.D., Waddle, J.A., Schumacher, J.M., and Lin, R. (2002). The aurora kinase AIR-2 functions in the release of chromosome cohesion in Caenorhabditis elegans meiosis. J. Cell Biol. *157*, 219–229.

Ruchaud, S., Carmena, M., and Earnshaw, W.C. (2007). Chromosomal passengers: conducting cell division. Nat. Rev. Mol. Cell Biol. *8*, 798–812.

Sokac, A.M., Co, C., Taunton, J., and Bement, W. (2003). Cdc42-dependent actin polymerization during compensatory endocytosis in Xenopus eggs. Nat. Cell Biol. *5*, 727–732.

Taieb, F.E., Gross, S.D., Lewellyn, A.L., and Maller, J.L. (2001). Activation of the anaphase-promoting complex and degradation of cyclin B is not required for progression from Meiosis I to II in *Xenopus* oocytes. Curr. Biol. *11*, 508–513.

Tatsumoto, T., Xie, X., Blumenthal, R., Okamoto, I., and Miki, T. (1999). Human ECT2 is an exchange factor for Rho GTPases, phosphorylated in G2/M phases, and involved in cytokinesis. J. Cell Biol. *147*, 921–928.

Tatsumoto, T., Sakata, H., Dasso, M., and Miki, T. (2003). Potential roles of the nucleotide exchange factor ECT2 and Cdc42 GTPase in spindle assembly in Xenopus egg cell-free extracts. J. Cell. Biochem. *90*, 892–900.

Terret, M.E., Wassmann, K., Waizenegger, I., Maro, B., Peters, J.M., and Verlhac, M.H. (2003). The meiosis I-to-meiosis II transition in mouse oocytes requires separase activity. Curr. Biol. *13*, 1797–1802.

Uzbekova, S., Arlot-Bonnemains, Y., Dupont, J., Dalbies-Tran, R., Papillier, P., Pennetier, S., Thelie, A., Perreau, C., Mermillod, P., Prigent, C., and Uzbekov, R. (2008). Spatio-temporal expression patterns of aurora kinases A, B, and C and cytoplasmic polyadenylation-element-binding protein in bovine oocytes during meiotic maturation. Biol. Reprod. *78*, 218–233.

Yuce, O., Piekny, A., and Glotzer, M. (2005). An ECT2-centralspindlin complex regulates the localization and function of RhoA. J. Cell Biol. *170*, 571–582.

Zou, H., McGarry, T.J., Bernal, T., and Kirschner, M.W. (1999). Identification of a vertebrate sister-chromatid separation inhibitor involved in transformation and tumorigenesis. Science *285*, 418–422.